

**Multi-Species Test of  
Ion Cyclotron Resonance Heating  
at High Altitudes**

by

A. M. Persoon<sup>1</sup>, W. K. Peterson<sup>2</sup>, M. André<sup>3</sup>, T. Chang<sup>4</sup>,  
D. A. Gurnett<sup>1</sup>, J. M. Retterer<sup>5</sup>, and G. B. Crew<sup>4</sup>

July 1997

<sup>1</sup> Dept. of Physics and Astronomy, University of Iowa, Iowa City, IA 52242

<sup>2</sup> Lockheed Space Science Lab., 3251 Hanover, Palo Alto, CA 94304

<sup>3</sup> Swedish Inst. of Space Physics, Umea, Sweden

<sup>4</sup> Center for Space Physics, Massachusetts Inst. of Technology, Cambridge, MA 02139

<sup>5</sup> Phillips Laboratory, PL/GPSM, 29 Randolph Road, Hanscom AFB, MA 01731

## ABSTRACT

Observations of ion distributions and plasma waves obtained by the Dynamics Explorer 1 satellite in the high-altitude, nightside auroral zone are used to study ion energization for three ion species. A number of theoretical models have been proposed to account for the transverse heating of these ion populations. One of these, the ion cyclotron resonance heating (ICRH) mechanism, explains ion conic formation through ion cyclotron resonance with broadband electromagnetic wave turbulence in the vicinity of the characteristic ion cyclotron frequency. The cyclotron resonant heating of the ions by low-frequency electromagnetic waves is an important energy source for the transport of ions from the ionosphere to the magnetosphere.

In this paper we test the applicability of the ICRH mechanism to three simultaneously heated and accelerated ion species by modelling the ion conic formation in terms of a resonant wave-particle interaction in which the ions extract energy from the portion of the broadband electromagnetic wave spectrum which includes the ion cyclotron frequency. Using a Monte Carlo technique we evaluate the ion heating produced by the electromagnetic turbulence at low frequencies and find that the wave amplitudes near the ion cyclotron frequencies are sufficient to explain the observed ion energies.

## I. INTRODUCTION

Observations of ion conics have been reported in the literature for more than twenty years (extensive review of transverse auroral ion acceleration in Klumpar [1986]; review of ion conic distributions in Dynamics Explorer data in Burch [1988]). The characteristic signature of an ion conic on a high-resolution, energy-time spectrogram is that of a cone-shaped distribution centered on the magnetic field direction. The cone-shaped distribution is attributable to a combination of transverse acceleration and adiabatic motion of the ions along inhomogeneous geomagnetic field lines.

A great number of theoretical models have been proposed to account for the transverse heating of these ion populations. Reviews of these theories can be found in Lysak [1986], Chang et al. [1988] and André and Chang [1993]. The problem with identifying the process of ion conic formation has not been the lack of theoretical models, but the lack of simultaneous wave and particle data on appropriate time scales. Because the postulated wave-particle interactions that create ion conics are mass-dependent, knowledge of the conic ion mass is essential.

Wave-particle interaction mechanisms have been advanced which have sought to explain the conic formation by means of wave-particle interactions involving lower hybrid waves and electromagnetic and electrostatic ion cyclotron waves, as well as other low frequency waves (see references in Crew et al. [1990], Retterer et al. [1989], Klumpar et al. [1986], and Peterson et al. [1988]). However, certain observations of ion conic distributions did not fit the previous wave-particle interaction models, due to the absence of the necessary wave modes and to the absence of any means to generate these waves [Winningham and Burch, 1984; Klumpar et al., 1984]. In addition to the lack of necessary wave modes to

generate conics, the two conic distributions in the Klumpar study were puzzling because the conic signature suggested a two-stage acceleration process acting on the ions in which the ions experience a low-altitude acceleration transverse to the geomagnetic field, followed by acceleration along the field line at higher altitudes in the magnetosphere. The two-stage acceleration process was invoked to explain the characteristic signature of these bimodal conics in which the ions are field-aligned at lowest energies but become conical at increasing energy with the flux and cone angle increasing with increasing energy [Klumpar et al., 1984]. Temerin [1986] found that any transverse bulk heating mechanism operating over a wide range of altitudes could, acting in concert with the mirror force, produce the characteristic combination of parallel acceleration and perpendicular heating.

Chang et al. [1986] and Retterer et al. [1987] studied the 81318 event of Winningham and Burch [1984] and proposed that the  $O^+$  ions had been transversely energized through a cyclotron resonant interaction with low frequency broadband electromagnetic turbulence. In this theory, the necessary waves would be generated by some remote magnetospheric or ionospheric process and would propagate to altitudes where the waves would relinquish some of their energy to the ions, resulting in the observed transverse acceleration. The low frequency electromagnetic turbulence, a potential source of energy for such a resonant interaction, is a frequent occurrence at low altitudes over the auroral zones [Gurnett et al., 1984]. Johnson et al. [1989] identified a plausible source of this turbulence in equatorially generated low frequency ion cyclotron waves. These waves propagate into the ion-heating region where the left-hand circularly polarized component of the waves resonates with the thermal oxygen ions [Horne and Thorne, 1990 and Rönmark and André, 1991].

Retterer et al. [1987] employed a Monte Carlo technique to model the quasi-linear diffusion of the heated ions and included the effect of the magnetic mirror force which continually converts perpendicular energy to parallel energy even as the ions are experiencing additional transverse acceleration [Temerin, 1986]. Thus the ion cyclotron heating (ICRH) mechanism could account for both the parallel and perpendicular acceleration components of the bi-modal distributions observed by Klumpar et al. [1984]. Retterer et al. [1987] successfully modeled  $O^+$  conics along auroral field lines mapping into the central plasma sheet, via cyclotron resonance with the observed electromagnetic turbulence. Norqvist et al. [1996] used a Monte Carlo simulation similar to that used by Retterer et al. [1987] to study ion heating in the dayside high-latitude magnetosphere. After testing several heating mechanisms, including particle interactions with waves over a range of frequencies from below the ion cyclotron frequency to above the lower hybrid frequency, Norqvist et al. [1996] found that the cyclotron resonant mechanism is the dominant ion heating mechanism, a result consistent with other studies in the dayside, high-latitude magnetosphere by the Dynamics Explorer 1 and Viking satellites [André et al., 1988, 1990].

Crew et al. [1990] developed an intensive theoretical treatment of energetic oxygen ion conic formation through ion cyclotron resonance with electromagnetic plasma turbulence. Crew and co-authors developed a two-parameter representation of an ion conic distribution in which the heating process is characterized by the velocity scale and a pitch angle scaling parameter of three well-defined  $O^+$  conic events. The conic form predicted by their algorithm and the ICRH theory was found to be in excellent agreement with the three conic

formations of energetic  $O^+$  conics previously discussed in Winningham and Burch [1984] and Klumpar et al. [1984].

In addition to  $O^+$  ion conic distributions, conic distributions of  $He^+$  ions are frequently observed in the earth's magnetosphere. So far, the ICRH theory has been successfully applied to a limited number of energetic  $O^+$  ion conic events. The success of the ICRH theory for these limited cases immediately raises questions concerning the general applicability of this mechanism to other ion species. This paper will address this issue by testing the general applicability of the ICRH mechanism to hydrogen, helium and oxygen conic distributions, observed simultaneously along low-latitude auroral and subauroral field lines in the nightside magnetosphere.

We will use the analytic technique employed first by Chang et al. [1986] and Retterer et al. [1987] and later by André et al. [1990] and Norqvist et al. [1996] to study the effects of resonant ion heating by broadband low-frequency waves. Previously, much of the work on the cyclotron resonance heating of ions has focused on the auroral and cusp/cleft regions where the more energetic and intense ion conics are frequently observed. However, magnetometer data also reveals the presence of field-aligned currents and strong  $E \times B$  drifts which complicate the ion orbits and the estimates of the ion heating. To investigate the applicability of the ICRH mechanism to lighter ion species, we have chosen examples of ion conic distributions from lower auroral and subauroral latitudes where field-aligned currents are weak or absent.

This study utilizes ion data from the Energetic Ion Composition Spectrometer (EICS) and wave data from the Plasma Wave Instrument (PWI) on the Dynamics Explorer 1 spacecraft. Dynamics Explorer 1 was launched in August of 1981 into an eccentric polar orbit with perigee and apogee geocentric radial distances of  $1.09 R_E$  and  $4.66 R_E$ , respectively. Data from the first three years of the Dynamics Explorer mission were screened to identify examples of helium conic distributions with simultaneous heating of hydrogen and oxygen ions. The study will focus on applying the ICRH mechanism to the heating of helium ions and will compare the modeling of the  $He^+$  ions with the models of the hydrogen and oxygen ion distributions, all using the analytic techniques of Chang et al. [1986], Retterer et al. [1987] and André et al. [1990] to show that the low-frequency wave spectra can effectively produce the observed ion conic distributions.

Observations from the Energetic Ion Composition Spectrometer (EICS) have been used to identify three events with helium conic distributions from high-latitude regions in the nightside magnetosphere where field-aligned currents are weak or absent. EICS is a high-resolution ion mass spectrometer, designed to measure the energy and pitch angle distributions of ions in a mass range of less than 1 amu/e to 150 amu/e in 64 mass channels. The energy range of the ions spans 0 eV (spacecraft potential) to 17 keV/e in 32 energy steps. The field of view of the instrument is perpendicular to the spacecraft spin axis and provides complete pitch angle coverage every spacecraft rotation (6 seconds). The instrument is described in detail by Shelley et al. [1981] and André et al. [1990].

Electric field spectrum measurements from the Plasma Wave Instrument (PWI) have been used to derive the power of the plasma waves in the vicinity of the ion cyclotron frequency. The PWI on Dynamics Explorer 1 has been described in detail in Shawhan et al. [1981]. The low frequency (below 8 Hz) electric field spectral density measurements are

obtained from the Fourier analysis of the time series dc electric field measurements. The dc electric field data have a frequency resolution of 0.33 Hz and a time resolution of 3 seconds. The instrument samples all orientations with respect to the local magnetic field [André et al., 1990]. The dc electric field measurements are obtained from the 200-m (tip-to-tip) electric antenna, oriented perpendicular to the spin axis. Signals from this same long-wire antenna are also processed by a pair of step-frequency receivers which sweep a frequency range of 1.78 Hz to 410 kHz once every 32 seconds. The resulting electric field amplitude measurements are displayed in frequency-time color spectrograms (with the wave amplitude encoded in the color bar) and in amplitude-frequency electric field spectral density plots.

## II. OBSERVATIONS AND ANALYSIS

Three examples of helium, oxygen and hydrogen conics have been selected for an analysis of the ion cyclotron resonance heating (ICRH) mechanism. The events were identified using the conic-finding technique described in Peterson et al. [1992].

Our objective is to show that the waves at the local ion cyclotron frequency possess sufficient energy to produce the observed ion heating for multiple ion species by comparing the ion energy inferred from the observed ion distribution to the theoretical ion energy derived from the wave power spectral density at the local ion cyclotron frequency. There are two established analytical methods for making this comparison. André et al. [1990] took advantage of the unique geophysical structure of the dayside cusp region where, under normal conditions, cold plasma drifts into a region characterized by intense wave power at the relevant ion cyclotron frequencies.

We have chosen to focus our attention on the nightside auroral field lines and adapt the technique developed by Crew et al. [1990]. This technique assumes that bulk ion motion is in a direction such that the ions are exposed to an essentially constant flux of plasma wave power at the relevant ion cyclotron frequencies. The ICRH method also assumes that the plasma wave power spectrum in the relevant frequency range has a slope and magnitude independent of altitude below the point of observation. The end product of the Crew et al. [1990] ICRH technique is a two-parameter representation of the ion distribution and the wave power.

Our initial approach to the comparison of the observed ion conic energies and those predicted by the ICRH theory was to use the full theoretical treatment discussed in the Crew et al. [1990] paper. The advantage of the full formulation of the ICRH theory is that it provides an analytical way to calculate the two characteristic ICRH parameters from moments of the measured ion distribution function and from characteristics of the plasma wave spectrum. The ICRH theory predicts that the two characteristic ICRH parameters calculated from the measured distribution functions should equal those calculated from the plasma wave spectrum. However, using the Crew et al. [1990] method to analyze  $\text{He}^+$  ion distributions proved to be unfeasible because the signal levels in the observed helium distributions were lower than anticipated, resulting in large uncertainties in the calculated parameters. The Crew et al. [1990] method could not be used to show that the predictions of the ICRH theory are consistent with observed plasma waves and ion distribution functions.

Rather than obtain characteristics of the ion distribution function from moments calculations, we estimated a single characteristic energy as outlined below. We compared this characteristic energy inferred from the ion distribution with the characteristic energy derived from the plasma wave power spectrum, using the analysis technique developed by Retterer et al. [1987]. Retterer et al. [1987] related two characteristics of the wave power spectral density, the magnitude and the slope of the wave spectral density at the local ion cyclotron frequency, to the predicted characteristic energy of an ion conic. We present and discuss the limitations of the method we used to calculate the characteristic energies from the measured ion distribution in parallel with the presentation of the data from the first of the three auroral zone crossings.

### March 5, 1983

The first ion conic event to be identified is taken from a nightside crossing of the auroral zone in the southern hemisphere on March 5, 1983. Plate 1 summarizes our observations of the ion distributions for this crossing and the associated plasma wave activity. The top three color panels display nine successive angle-energy flux distributions from the Energetic Ion Mass Spectrometer (EICS) for the 14-minute interval beginning at 23:42 UT on March 5.  $H^+$ ,  $He^+$  and  $O^+$  ion fluxes for the nine successive ion distributions are presented in an angle-energy postage stamp format. Ion fluxes for each 96-second interval are presented with ion pitch angles from 0 to 180 degrees as the ordinate (vertical axis) and energy from 10 eV/e to 17 keV/e as the abscissa (horizontal axis). Ion fluxes in units of  $(\text{cm}^2\text{-s-sr-keV})^{-1}$  at each energy-pitch angle position are encoded, using the color bar on the right side of the ion panels. The ions, flowing up magnetic field lines in the southern hemisphere, have pitch angles of 0 degrees in this plot format. It should also be noted that the EICS instrument mode, used in all of the intervals presented in this paper, obtained data for only one energy setting per spin (every 6 seconds). The order in which ion energies were sampled was not monotonic and 16 spins (96 seconds) were required to obtain a complete ion energy-angle distribution. The striped nature of the data for all three ions in the seventh interval at approximately 23:53 UT are the result of a significant change in the intensity and angular distribution of the ion populations during this sampling interval. We refer to this effect as time aliasing of the data.

Helium conic distributions at low energies appear near the equatorward edge of the nightside auroral zone at 23:47 UT (in the fourth interval) and at 23:50 UT (in the sixth interval) in the low energy bins. Simultaneously, well-defined  $O^+$  and  $H^+$  conics are observed at 23:47 UT (fourth interval). A second interval, showing a weaker  $O^+$  conic distribution and a simultaneous intense  $H^+$  conic distribution, occurs in the eighth interval at 23:53 UT.

Also presented in Plate 1 are spectrograms of simultaneously acquired plasma wave data. The bottom two color panels present plasma wave data from the electric field antennas of the Plasma Wave Instrument (PWI) on Dynamics Explorer 1. The fourth color panel presents the power spectral density obtained from the Fourier analysis of the time series dc electric field measurements made by the PWI instrument. The power spectra were obtained

from time series electric field measurements made in the satellite spin plane which samples all orientations with respect to the local magnetic field [André et al., 1990]. This panel presents the electric field power spectral density (in units of  $V/m^2/Hz$ , encoded on the color bar to the right of the panel) over the frequency range from 0 to 8 Hz. The frequency axis on this panel is linear.

The electric field measurements in the fourth panel indicate an intense increase in the wave power at low frequencies corresponding to the occurrence of the weak helium conics. The spectrogram illustrates the onset of intense low-frequency wave activity beginning at 23:50 UT and continuing until 23:52 UT. The oxygen and helium cyclotron frequencies (1.6 Hz and 5 Hz, respectively) are embedded within this intense wave activity. This interval of intense low-frequency wave activity correlates with the less intense  $He^+$  conic distribution at 23:50 UT in the low energy bins. Wave activity in the fourth interval is intermittent and not highly correlated with the occurrence of the ion conic distributions.

The bottom color panel presents the electric field measurements for the frequency range from 1 Hz to 410 kHz obtained from the Low Frequency Correlator (LFC) and the Sweep Frequency Receiver (SFR) of the PWI instrument. The plasma wave spectral density is given in units of  $V^2/m^2/Hz$  encoded on the color bar to the right of the panel. The strong emissions above 100 kHz observed throughout this interval are auroral kilometric radiation (AKR). The black intervals at either end of the spectrogram are artifacts of the data display. The 32-second instrumental cycle time of the SFR is readily apparent from the striped nature of the spectrum at low frequencies. This striped appearance is indicative of substantial changes in the in situ plasma wave spectrum on time scales short compared to the 32-second SFR cycle time.

The ion conics in the top three panels occur during a period of intense wave activity below 100 Hz which extends throughout much of this interval. The intense wave activity ends abruptly in the seventh interval just prior to the intensification in the  $H^+$  distribution at 23:53 UT. The hydrogen cyclotron frequency (approximately 23 Hz) is embedded within this intense low frequency wave activity. This type of broadband low-frequency turbulence is commonly observed along nightside auroral field lines [Gurnett et al., 1984].

Our goal is to compare characteristic ion energies perpendicular to the local magnetic field predicted by the ICRH theory with those inferred from direct measurement by the EICS instrument. The bottom two panels of Plate 1 display the characteristic ion energy perpendicular to the magnetic field line inferred from the measured  $He^+$ ,  $O^+$  and  $H^+$  distribution functions and the predicted perpendicular energy calculated from the characteristics of the plasma wave spectral density spectrum [Retterer et al., 1987]. Before entering into a detailed comparison of the measured and predicted perpendicular energies, we need to examine more closely how they were determined.

In order to reduce the effects of time aliasing caused by significant variations in both the ion and plasma wave power distributions on time scales short compared to the 96-second EICS measurement interval, we have chosen to calculate characteristic energies for 48 seconds rather than 96-second intervals. The order in which the EICS energy steps are acquired is such that a majority of the EICS low energy steps (those with energies below 1 keV) were acquired in alternate 48-second intervals. It is the characteristic perpendicular

energy from these 48-second intervals, not the full 96-second EICS instrumental cycle time, that is presented in the bottom two panels of Plate 1.

Figure 1 presents representative plasma wave spectra and  $\text{He}^+$  distribution functions for the three specific 48-second intervals centered on the times indicated during the nightside auroral zone crossing on March 5, 1983. We focus first on the plasma wave data in the upper left panel. Data are presented for the three intervals indicated. The  $\text{O}^+$  and  $\text{He}^+$  cyclotron frequencies are indicated by arrows (1.5 and 6 Hz, respectively). The  $\text{H}^+$  cyclotron frequency was approximately 23 Hz during the auroral zone crossing. Retterer et al. [1987] relate the magnitude and slope of the wave power spectral density at the ion cyclotron frequency to a characteristic energy of the ion distribution function. For the three times indicated, ICRH theory predicts characteristic energies of 25, 38, and 55 eV, respectively (assuming that 10% of the full wave spectrum is left-hand polarized). The predicted characteristic energies for  $\text{He}^+$  and  $\text{O}^+$  determined in this way are presented in the bottom panel of Plate 1. Even though we do not expect  $\text{H}^+$  ions to be energized primarily by the ICRH mechanism, we have interpolated the SFR power spectral density in frequency and time to obtain estimates of a characteristic  $\text{H}^+$  energy as if the only process acting on the dominant  $\text{H}^+$  ions were ion cyclotron resonance heating. These data are also presented in the bottom panel of Plate 1.

Contour plots of the measured  $\text{He}^+$  velocity space distributions for the same three time intervals are presented in the remaining three panels of Figure 1. The circles of small dots centered on the origin indicate the velocities parallel and perpendicular to the local magnetic field at which  $\text{He}^+$  ions were sampled. Because the EICS instrument mode requires 96 seconds to cycle through the 15 energies and a background measurement, determination of a characteristic energy is complicated by changes in the overall flux level during the full instrument cycle. To minimize this distortion we have used data from 8 of the energy steps acquired within 48 seconds. The 4 innermost circles of dots in the contour plots were obtained when EICS was sampling  $\text{He}^+$  with energies of 60, 230, 870 and 1120 eV, respectively. The outermost circle of dots is an artifact of the contouring routine which also had inputs of  $\text{He}^+$  fluxes at 3.7, 5.0, 12.7 and 17.0 keV, corresponding to  $\text{He}^+$  velocities greater than 300 km/s. Presented in the panels labeled 1-3 are contours of the maximum of the EICS one count per interval response and the measured value of the  $\text{He}^+$  velocity space density. Contours are given in units of the log (base 10) of the distribution function in units of  $\text{km}^6/\text{sec}^3$ . In this representation, data below the one count per measurement interval level appear as circular contours centered on zero velocity. The  $\text{He}^+$  conic angular distributions are such that they appear to have a non-zero velocity parallel to the magnetic field line at the maximum of the distribution function--that is, the  $\text{He}^+$  angular distributions appear to be the type that are created by ion cyclotron resonance heating as described by Chang et al [1986]. Note that the contouring routine smoothly interpolates over the rather wide velocity gap between the 230 and 870 eV measurements.

The characteristic  $\text{He}^+$  energies perpendicular to the local magnetic field line for the three intervals in Figure 1 are 18, 104, and 21 eV, respectively. Operationally they were determined graphically from the contour plots. A quasi-hyperbolic shaped line of maximum velocity space density (called a conic path) was hand-drawn on each contour. Lines were then drawn parallel to the  $V_{\parallel} = 0$  axis between intersections of the conic path and the



contours. The half length of the lines connecting the two branches of the conic path, expressed as a velocity  $f$ , was used, along with the value of the velocity space density corresponding to that contour level, as inputs to a routine to fit the function

$$f = f_0 \cdot \exp(-mv^2/2 \cdot \kappa T) \quad .$$

There are very obvious limitations to this method of determining a characteristic perpendicular energy from the EICS data. The  $\text{He}^+$  data in the three intervals presented in Figure 1 correspond to an time when the characteristic flux, energy, and angular distribution of the ions changed from a cool ion conic of indeterminate angular width (interval 1) to a mid-energy conic with a wide angular width (interval 2) to a slightly less energetic conic with a relatively narrow angular width. Similar patterns in the  $\text{O}^+$  and  $\text{H}^+$  ion distributions can be seen in the color spectrogram postage stamp angle-energy data for these intervals in Plate 1. As noted above, we have not included  $\text{He}^+$  fluxes at 430 and 650 eV, which were sampled in the time between interval 1 and 2. Omission of these data from the contour algorithm, coupled with the few counts detected in the 870 eV  $\text{He}^+$  fluxes that were included, results in contours that are apparently biased to higher velocities. Inclusion of the 430 and 650 eV  $\text{He}^+$  data in the contour algorithm produces contours that do not have the regular quasi-hyperbolic shape apparent in the data for intervals 2 and 3. Examination of the color spectrograms shows that interval 2 data were obtained on or near a boundary in the background  $\text{H}^+$  ion distribution. Prior to interval 2 the hot, quasi-isotropic component of the  $\text{H}^+$  plasma is relatively more intense than it was after interval 2.

Some additional information about the plasma environment is available from the Dynamics Explorer 1 magnetometer. A weak (approximately  $0.5 \mu\text{A}/\text{m}^2$ ) downward-directed field-aligned current was detected by the Dynamics Explorer 1 magnetometer at 23:46:25 UT at or near the boundary in the background  $\text{H}^+$  ion distribution. The region with a relatively less intense hot, quasi-isotropic  $\text{H}^+$  distribution extends to about 23:51 UT where a weaker (approximately  $0.25 \mu\text{A}/\text{m}^2$ ) pair of field-aligned currents are detected. Between 23:46:45 UT and 23:51:45 UT the magnetometer shows an increase of 37 nT in the E-W magnetic field corresponding to a very weak, large-scale, downward field-aligned current less than  $0.1 \mu\text{A}/\text{m}^2$ . Prior to 23:46 UT no significant change in the E-W magnetic field was detected. After 23:52 UT the magnetometer detected a weak, upward, large-scale, field-aligned current of comparable magnitude to the weak, downward current noted above.

The most striking feature of Plate 1 is the agreement of the measured and predicted  $\text{He}^+$  characteristic perpendicular energies between 23:48 UT and 23:52 UT and the disagreement of the predicted and measured  $\text{H}^+$  and  $\text{O}^+$  characteristic energies. We defer discussion of the comparison of measured and predicted characteristic perpendicular energy until after presentation of data obtained in two other crossings of the auroral zone.

**February 16, 1982**

The second interval on February 16, 1982 was selected by the EICS conic-finding code as the most intense example of a helium conic distribution. Since helium conics are typically weak distributions, this example is a particularly compelling one to analyze. Plate 2 presents ion and plasma wave data and inferred characteristic energies in the same format as Plate 1. The data presented in Plate 2 were obtained near midnight in magnetic local time but at slightly higher altitudes and invariant latitudes than those presented in Plate 1. The six successive angle-energy flux distributions for  $H^+$  show a distribution characterized by a cool (i.e., low energy) upflowing population that increases in intensity and then decreases. These spectra were obtained in the northern hemisphere, so upflowing ions have pitch angles in the 90-180 degree range. The  $H^+$  distribution also has a hot quasi-isotropic component that gradually gets less energetic during the interval, as evidenced by the black color for the highest energy steps in the final  $H^+$  postage stamp display. The black color indicates that the observed fluxes are at or below the instrumental threshold of  $10^3$  ions/(cm<sup>2</sup>-ss-keV). Both the  $He^+$  and  $O^+$  postage stamps display well-defined conic distributions for the interval near 18:50 UT. Following the method described above, we determined characteristic perpendicular energies of 108 eV and 184 eV for the  $He^+$  and  $O^+$  distributions respectively. The angular width of the  $He^+$  conic is narrower in the following interval, resulting in a lower characteristic perpendicular energy (63 eV). The  $O^+$  distribution in the next interval retains most of the angular width, but the decline in the flux with energy is stronger. This also results in a lower characteristic perpendicular energy (113 eV). The limitation in our method to determine a characteristic perpendicular energy for  $He^+$  shows up again in the last interval (18:55 UT) where a few signal counts in the 870 eV channel bias the energy to an unrealistically high value.

The plasma wave data presented in Plate 2 are characterized by auroral kilometric radiation above 100 kHz, an intensification of the low frequency (less than 1 kHz) wave power shortly after 18:48 UT, fairly constant wave power in the 0-1 Hz range and rapidly (compared to ion measurement times) fluctuating wave power spectra before 18:48 UT. The  $He^+$  cyclotron frequency for this interval was near 2.6 Hz and the  $O^+$  cyclotron frequency for this interval was at approximately 0.7 Hz. An examination of the very low frequency wave electric field data in the fourth panel of Plate 2 shows intense wave activity at the oxygen cyclotron frequency throughout the first three intervals where the intense oxygen conic distributions are seen. However, although the wave power at the  $O^+$  cyclotron frequency was relatively constant in magnitude throughout this interval, there are rapid variations in the wave power with time and frequency for all frequencies above 1 Hz. Both the wave power and the changes in the wave power with increasing frequency at the  $He^+$  and  $H^+$  ion cyclotron frequencies fluctuate rapidly on the time scales required for the ion measurements, so the comparison between the measured and predicted perpendicular energies from the ICRH theory is not expected to be a good test of the ICRH mechanism, compared to the data presented in Plate 1.

The Dynamics Explorer 1 magnetometer data provide some additional information about the plasma environment on February 16. A pair of weak (approximately  $0.5 \mu A/m^2$ ), oppositely directed, field-aligned currents was detected at 18:48 UT, corresponding to the

onset of fluctuations in the plasma wave power above 1 Hz. From 18:48 UT to 18:54 UT, small-scale, field-aligned currents of both polarities were observed with magnitudes in the range 0.3 to 0.9  $\mu\text{A}/\text{m}^2$ .

The most striking feature of the data presented in Plate 2 are the high energies of the both measured and predicted characteristic perpendicular energies for all of the ion species. There is good agreement between the measured and predicted perpendicular energies for both the  $\text{He}^+$  (1850 UT) and the  $\text{O}^+$  (1848 UT) ion distributions.

## April 21, 1982

This event on April 21, 1982 has been included to show an example of localized ion heating. Plate 3 presents ion and plasma wave data in the same format as Plates 1 and 2. The plasma wave data in this interval (panels 4 and 5) are less intense than they were in the two previous examples. The main difference in the plasma wave spectra, however, is the emission feature near 2 Hz (panel 4), slightly above the  $\text{He}^+$  cyclotron frequency (1 Hz). The plasma wave emission feature was observed prior to 00:04 UT, but the EICS instrument was not turned on until 00:04 UT on this day. Emission features in the few Hz range have been presented and discussed by Anderson and Fuselier [1994].

A distinct upflowing  $\text{He}^+$  conic distribution can be seen in the postage stamp display near 00:06 UT in the second color panel of Plate 3. The helium conic correlates well with the intense line emission in the plasma wave spectrogram near the helium cyclotron frequency (panel 4) through 00:09 UT. Anderson and Fuselier [1994] have shown that, in the presence of electromagnetic ion cyclotron waves where the wave frequency approaches the helium cyclotron frequency, helium ions are strongly heated in a gyroresonant interaction with the waves. These ions have a characteristic distribution with maximum fluxes occurring at intermediate pitch angles between the field-aligned and the perpendicular direction. The April 21 line emission just above the helium cyclotron frequency and the simultaneous heating of the helium ions at intermediate pitch angles is in good agreement with the results of the Anderson and Fuselier study.

Here we focus on the relationship between the observed ion energy perpendicular to the magnetic field to see if the observed energies are consistent with those predicted by the ICRH theory. Detailed examination of contour plots from the five intervals for which 48-second EICS accumulations were obtained shows that superimposed on the warm (greater than 1 keV) quasi-isotropic  $\text{H}^+$ ,  $\text{O}^+$  and  $\text{He}^+$  distributions are well-defined, low energy ( $< 1$  keV) ion conic distributions. The characteristic perpendicular energies obtained from these contours are presented in panel 6 of Plate 3.

The interval presented in Plate 3 is at a slightly lower latitude and earlier local time than the previous two examples. The ion distributions displayed in the top three panels are more characteristic of those found in the plasmopause region than the auroral region, as evidenced by the lack of a distinct signature of low energy (just above the 10 eV EICS energy threshold) ions flowing up magnetic field lines. The Dynamics Explorer magnetometer data for this interval show a large-scale, downward, field-aligned current from 00:03:30 UT to approximately 00:09:30 UT. From 00:09:30 UT to 00:11:45 UT, the

current was slightly more intense and upward. After 00:11:45 UT, a downward current sheet of similar intensity was observed. It is interesting to note that the boundaries of these weak, field-aligned currents occur at the same time as intensifications in the low frequency ( $< 8$  Hz) plasma wave spectra.

The most striking feature of the data presented in Plate 3 is the apparent agreement between the measured and predicted  $H^+$  perpendicular energies between 00:07 UT and 00:11 UT, compared with the apparent disagreement for  $He^+$  and  $O^+$ . The ICRH hypothesis for  $He^+$  ions in gyroresonant interaction with the electromagnetic ion cyclotron waves applies to broad spectral peaks with wave amplitude and frequency variation independent of altitude, assumptions not valid for line emission events.

### III. DISCUSSION AND CONCLUSIONS

We have tested the importance of the ion cyclotron heating mechanism in the magnetosphere by using ion mass spectrometer data and wave observations from the Dynamics Explorer 1 satellite. As in earlier investigations, we find that the ICRH mechanism seems to be an important ion energization mechanism in the magnetosphere. In the events we have studied, there is general correlation between the waves around the ion cyclotron frequencies and the observed ion heating. The wave amplitudes during these events are large enough to cause the observed ion energies. The ICRH mechanism has been tested in previous studies, typically for the heating of  $O^+$  ions, and has been shown to be a viable heating mechanism in the auroral regions. In this study, we have investigated the simultaneous heating of three ion species,  $H^+$ ,  $He^+$  and  $O^+$ . We have been able to show that the observed wave amplitudes in three different frequency ranges are sufficient to produce the observed ion heating in two of the three events.

During the first two events when all three ion species are heated, there is enough wave power around all three cyclotron frequencies to produce the observed heating, although the predicted and measured ion energies are not consistently comparable in detail for all three ion species. On April 21, 1982 only  $He^+$  is heated and there is significant wave power only around the  $He^+$  cyclotron frequency. And, although the comparison of the predicted and measured ion energies using the ICRH technique are not entirely convincing for this event, no other obvious energy sources, such as lower hybrid waves, are observed. All of our observations indicate that the ICRH mechanism is a probable and significant factor in the observed ion heating during these events.

Although ICRH seems to be a major heating mechanism during these events, several questions remain. It is not obvious why the different ion species should have approximately the same energy, often within a factor of two. And there is typically a lot more wave energy available at the lowest frequencies (around a few Hz) than is necessary for cyclotron resonance heating of the ions. This would indicate that a smaller fraction of the electric field spectral density at these frequencies would seem to correspond to left-hand polarized waves. (We used a conservative fraction of 10% for the left-hand polarized waves in our analysis.) Or it could suggest that the wave polarization changes with frequency, although the details of these broadband low-frequency waves are not known.

There are other potential energy sources for the observed ion heating and acceleration in the auroral regions (see references in Crew et al. [1990]). Some frequently observed sources include particle beams and sharp gradients. However, no obvious local sources are observed during these three events.

One potential energy source which can complicate efforts to assess the relative importance of the ion cyclotron heating mechanism are field-aligned currents (FACs). FACs can generate electrostatic ion cyclotron waves which, in turn, are capable of heating the ions. Magnetometer data from Dynamics Explorer 1 [Farthing et al., 1981] was examined to locate and evaluate the strength of the field-aligned current activity during these three events and to indirectly determine the importance of the ion heating via electrostatic ion cyclotron waves. Typically the observed ion heating and the low frequency wave amplitudes correlated with the conic distributions along boundaries between relatively weak, oppositely-directed, large-scale FACs. The most intense ion heating in the first event, for example, occurs near a boundary between oppositely-directed, weak (less than  $0.5 \mu\text{A}/\text{m}^2$ ), large-scale FACs. Relatively intense (greater than  $0.5 \mu\text{A}/\text{m}^2$ ) currents are observed in these same regions but they are not symmetrically located with respect to the observed wave energy or the ion transverse energy. This would suggest that the weak currents and the possible presence of electrostatic ion cyclotron waves would not contribute significantly to the observed ion heating in the March 23 event.

During the second event, the broad peaks in the characteristic energies of all three ion species again occur at the boundary between two relatively weak (approximately  $0.5 \mu\text{A}/\text{m}^2$ ), oppositely-directed, large-scale, field-aligned current systems. Although the currents are not strong, the boundary between the oppositely-directed currents does correspond to rapid variations in the wave power in time and frequency for all frequencies greater than 1 Hz. Only in the oxygen cyclotron frequency range does the wave power remain constant in magnitude. Since these wave variations occur on short time scales comparable to the time scales in the EICS ion measurements, the analysis of the observed ion heating in this event did not provide a definitive test of the ICRH mechanism.

In the third event, neither the large- or small-scale currents identified in the magnetometer data have features centered on the region of the most intense  $\text{He}^+$  energization. As discussed previously, this event is an example of localized ion heating by a plasma wave line emission just above the helium cyclotron frequency. However, the ICRH technique fails to deliver a solid correlation between the predicted and measured ion energies because the technique requires broad wave spectral peaks and an assumption that the wave amplitude and frequency variations are independent of altitude. Since these assumptions are not valid for line emissions, this event was not a good candidate for the validation of the ICRH technique, even though ion heating via resonance with the ion cyclotron waves was certainly indicated by the plasma wave spectrum in the vicinity of the helium cyclotron frequency.

Many ion energization mechanisms are, in principle, viable mechanisms for producing the observed ion heating and more than one mechanism is probably operating in the terrestrial magnetosphere. For example, in addition to the ICRH mechanism, there are reports of ion energization by wave-particle interactions with lower hybrid waves [Retterer et

al., 1986; 1994; Eliasson et al., 1994]. Furthermore, a combination of ICRH and lower hybrid heating can be important [André et al., 1994].

Since other mechanisms contribute to ion heating in the magnetosphere, it does not seem to be meaningful to try to identify a single exclusive ion energization mechanism. The correlation between the observed ion heating in these three examples and the wave energy at the characteristic ion cyclotron frequency available to cause the ion heating clearly indicates that the ICRH mechanism is a significant ion heating mechanism in the magnetosphere.

## ACKNOWLEDGEMENTS

We wish to thank J. A. Slavin for providing the analysis and interpretation of the Dynamics Explorer magnetometer data. We also thank J. H. Dowell and Wei Feng for their work in software development that has been so essential in this study. This research has been funded by NASA Grant NAGW-3576.

## REFERENCES

- Anderson, B. J., and S. A. Fuselier, Response of thermal ions to electromagnetic ion cyclotron waves, *J. Geophys. Res.*, **99**, 19,413, 1994.
- André, M., H. Koskinen, L. Matson, and R. Erlandson, Local transverse ion energization in and near the polar cusp, *Geophys. Res. Lett.*, **15**, 107, 1988.
- André, Mats, G. B. Crew, W. K. Peterson, A. M. Persoon, C. J. Pollock, and M. J. Engebretson, Ion heating by broadband low-frequency waves in the cusp/cleft, *J. Geophys. Res.*, **95**, 20,809, 1990.
- André, M., and T. Chang, Ion heating perpendicular to the magnetic field, in *Physics of Space Plasmas*, Vol. 12, Scientific Publishers Inc., Cambridge, MA, 35, 1993.
- André, Mats, Patrik Norqvist, Andris Vaivads, Lars Eliasson, Olle Norberg, Anders I. Eriksson and Bengt Holback, Transverse ion energization and wave emissions observed by the Freja satellite, *Geophys. Res. Lett.*, **21**, 1915, 1994.
- Burch, . L., Energetic particles and currents: Results from Dynamics Explorer, *Rev. Geophys.*, **26**, 215, 1988.
- Chang, T., G. B. Crew, N. Hershkowitz, J. R. Jasperse, J. M. Retterer, and J. D. Winningham, Transverse acceleration of oxygen ions by electromagnetic ion cyclotron resonance with broad band left-hand polarized waves, *Geophys. Res. Lett.*, **13**, 636, 1986.

- Chang, T., G. B. Crew, and J. M. Retterer, Electromagnetic tornadoes in space: Ion conics along auroral field lines generated by lower hybrid waves and electromagnetic turbulence in the ion cyclotron range of frequencies, *Computer Physics Communications*, 49, 61, 1988.
- Crew, G. B., Tom Chang, J. M. Retterer, W. K. Peterson, D. A. Gurnett, and R. L. Huff, Ion cyclotron resonance heated conics: Theory and observations, *J. Geophys. Res.*, 95, 3959, 1990.
- Eliasson, L., M. André, A. Eriksson, P. Norqvist, O. Norberg, R. Lundin, B. Holback, H. Koskinen, H. Borg, and M. Boehm, Freja observations of heating and precipitation of positive ions, *Geophys. Res. Lett.*, 21, 1911, 1994.
- Farthing, W. H., M. Sugiura, B. G. Ledley, and L. J. Cahill, Jr., Magnetic field observations on DE-A and DE-B, *Space Sci. Instrum.*, 5, 551, 1981.
- Gurnett, D. A., R. L. Huff, J. D. Menietti, J. L. Burch, J. D. Winningham, and S. D. Shawhan, Correlated low-frequency electric and magnetic noise along the auroral field lines, *J. Geophys. Res.*, 89, 8971, 1984.
- Horne, R. B., and R. M. Thorne, Ion cyclotron absorption at the second harmonic of the oxygen gyrofrequency, *Geophys. Res. Lett.*, 17, 2225, 1990.
- Johnson, J. R., Tom Chang, G. B. Crew, and Mats André, Equatorially generated ULF waves as a source for the turbulence associated with ion conics, *Geophys. Res. Lett.*, 16, 1469, 1989.
- Klumpar, D. M., W. K. Peterson, and E. G. Shelley, Direct evidence for two-stage (bimodal) acceleration of ionospheric ions, *J. Geophys. Res.*, 89, 19,779, 1984.
- Klumpar, D. M., A digest and comprehensive bibliography on transverse auroral ion acceleration, in *Ion Acceleration in the Magnetosphere and Ionosphere*, *Geophysical Monograph Series*, Vol. 38, ed. by Tom Chang, M. K. Hudson, J. R. Jasperse, R. G. Johnson, P. M. Kintner, M. Schulz, and G. B. Crew, pp. 389, American Geophysical Union, Washington, DC, 1986.
- Lysak, R. L., *Ion Acceleration by wave-particle interaction*, in *Ion Acceleration in the Magnetosphere and Ionosphere*, *Geophysical Monograph Series*, Vol. 38, ed. by Tom Chang, M. K. Hudson, J. R. Jasperse, R. G. Johnson, P. M. Kintner, M. Schulz, and G. B. Crew, pp. 261, American Geophysical Union, Washington, DC, 1986.
- Norqvist, Patrik, Mats André, Lars Eliasson, Anders I. Eriksson, Lars Blomberg, Hermann Luhr, and James H. Clemmons, Ion cyclotron heating in the dayside magnetosphere, *J. Geophys. Res.*, Vol. 101, 13,179, 1996.

- Peterson, W. K., E. G. Shelley, S. A. Boardsen, D. A. Gurnett, B. G. Ledley, M. Suguira, T. E. Moore, and J. H. Waite, Transverse ion energization and low-frequency plasma waves in the mid-altitude auroral zone: A case study, *J. Geophys. Res.*, **93**, 11,405, 1988.
- Peterson, W. K., H. L. Collin, M. F. Doherty, and C. M. Bjorklund,  $O^+$  and  $He^+$  restricted and extended (bi-modal) ion conic distributions, *Geophys. Res. Lett.*, **19**, 1439, 1992.
- Retterer, J. M., T. Chang, and J. R. Jasperse, Ion acceleration by lower hybrid waves in the supraauroral region, *J. Geophys. Res.*, **91**, 1609, 1986.
- Retterer, J. M., T. Chang, G. B. Crew, J. R. Jasperse, and J. D. Winningham, Monte Carlo modeling of ionospheric oxygen acceleration by cyclotron resonance with broad-band electromagnetic turbulence, *Phys. Rev. Lett.*, **59**, 148, 1987.
- Retterer, J. M., T. Chang, and J. R. Jasperse, Particle acceleration by intense auroral VLF turbulence, in *Physics of Space Plasmas*, edited by Tom Chang, G. B. Crew and J. R. Jasperse, Scientific Publishers Inc., Cambridge, MA, 119, 1989.
- Retterer, J. M., Tom Chang, and J. R. Jasperse, Transversely accelerated ions in the topside ionosphere, *J. Geophys. Res.*, **99**, 13,189, 1994.
- Rönnmark, K., and M. André, Convection of ion cyclotron waves to ion heating regions, *J. Geophys. Res.*, **96**, 17,573, 1991.
- Shawhan, S. D., D. A. Gurnett, D. L. Odem, R. A. Helliwell, and C. G. Park, The plasma wave and quasi-static electric field instrument (PWI) for Dynamics Explorer-A, *Space Sci. Instrum.*, **5**, 535, 1981.
- Shelley, E. G., D. A. Simpson, T. C. Sanders, E. Hertzberg, H. Balsiger, and A. Ghielmetti, The energetic ion composition spectrometer (EICS) for the Dynamics Explorer-A, *Space Sci. Instrum.*, **5**, 443, 1981.
- Temerin, M., Evidence for a large bulk ion heating region, *Geophys. Res. Lett.*, **13**, 1059, 1986.
- Winningham, J. D. and J. L. Burch, Observation of large scale ion conic generation with DE-1, in *Physics of Space Plasmas (1982-4)*, SPI Conference Proceedings and Reprint Series, No. 5, edited by J. Belcher, H. Bridge, T. Chang, B. Coppi, and J. R. Jasperse, pp. 137-158, Scientific Publishers, Inc., Cambridge, MA, 1984.



### Plate and Figure Captions

- Plate 1.** Plate 1 summarizes the observed ion distributions and associated plasma wave activity for the nightside auroral zone crossing in the southern hemisphere on March 5, 1983. Each of the top three panels displays nine successive, 96-second, angle-energy flux distributions in a postage stamp format. Ion fluxes are presented with pitch angles from 0 to 180 degrees and energy from 10 eV/e to 17 keV/e. The fourth color panel presents the wave power spectral density from 0 to 8 Hz obtained from the Fourier analysis of the time series dc electric field measurements. The fifth color panel presents the PWI electric field measurements from 1 Hz to 410 kHz with the plasma wave spectral density encoded in the color bar. The bottom two panels display the characteristic ion energy perpendicular to the magnetic field inferred from the measured ion distribution function (sixth panel) and the predicted perpendicular energy calculated from characteristics of the plasma wave power spectrum (bottom panel). The data indicate a good correlation between the measured and predicted  $\text{He}^+$  characteristic perpendicular energies between 23:48 UT and 23:52 UT.
- Plate 2.** Plate 2 presents the ion and plasma wave data and the inferred characteristic ion energies in the same format as Plate 1 for an auroral zone crossing near local midnight in the northern hemisphere on February 16, 1982. The data indicate high characteristic perpendicular energies for all three ion species and a good correlation between the measured and predicted perpendicular energies for both  $\text{He}^+$  at 1850 UT and  $\text{O}^+$  at 1848 UT.
- Plate 3.** Plate 3 presents the ion and plasma wave data and the inferred characteristic ion energies in the same format as Plate 1 for a nightside auroral zone crossing in the northern hemisphere on April 21, 1982. The data indicate a good correlation between the measured and predicted  $\text{H}^+$  perpendicular energies from 00:07 UT until 00:11 UT, but poor correlations for the  $\text{He}^+$  and  $\text{O}^+$  measured and predicted perpendicular energies.
- Figure 1.** Figure 1 presents representative plasma wave spectra and  $\text{He}^+$  distribution functions for three specific 48-second intervals centered on 23:45:24 UT, 23:47:00 UT and 23:48:36 UT for the nightside auroral zone crossing on March 5, 1983.



MARCH 5, 1983

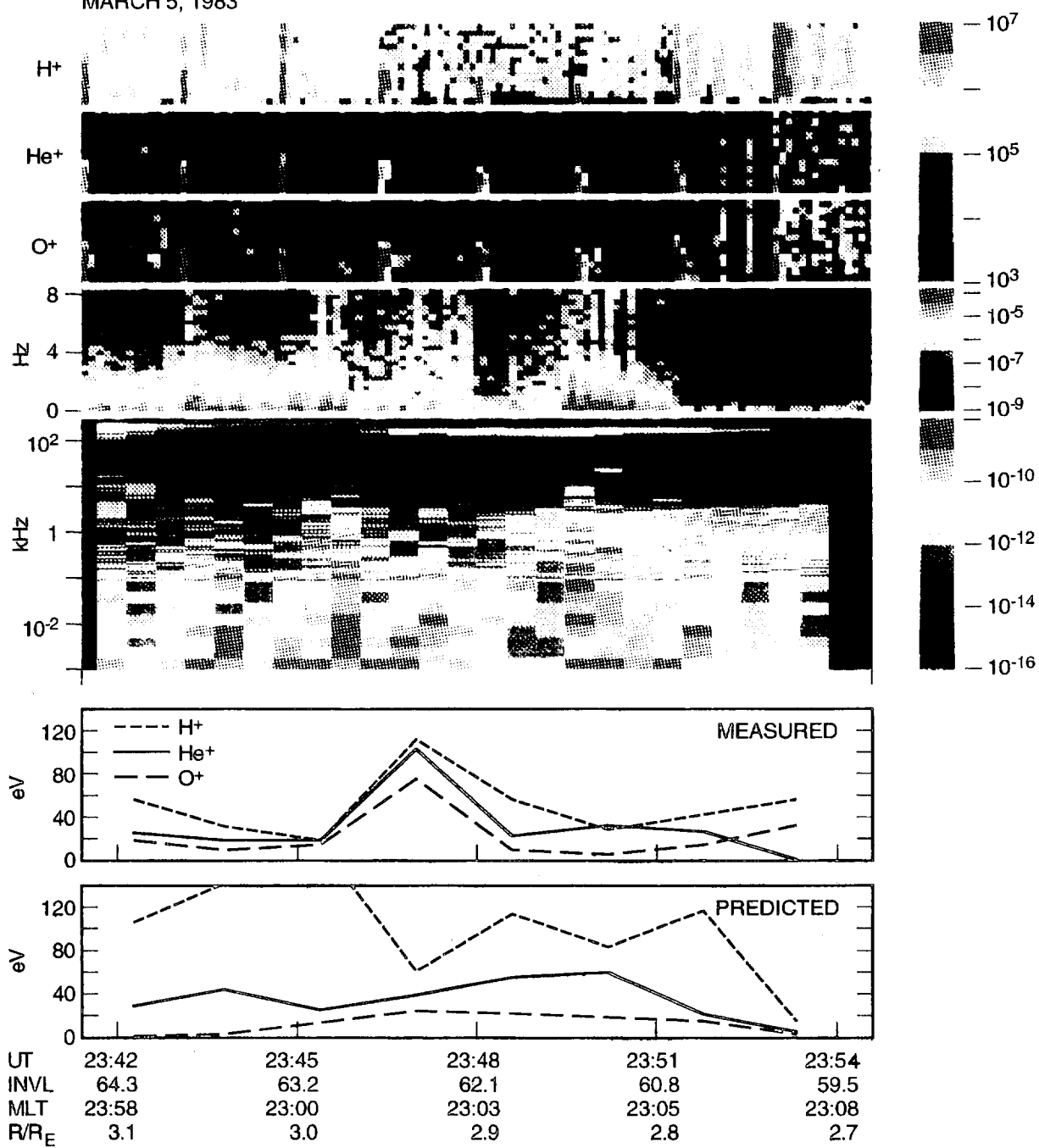
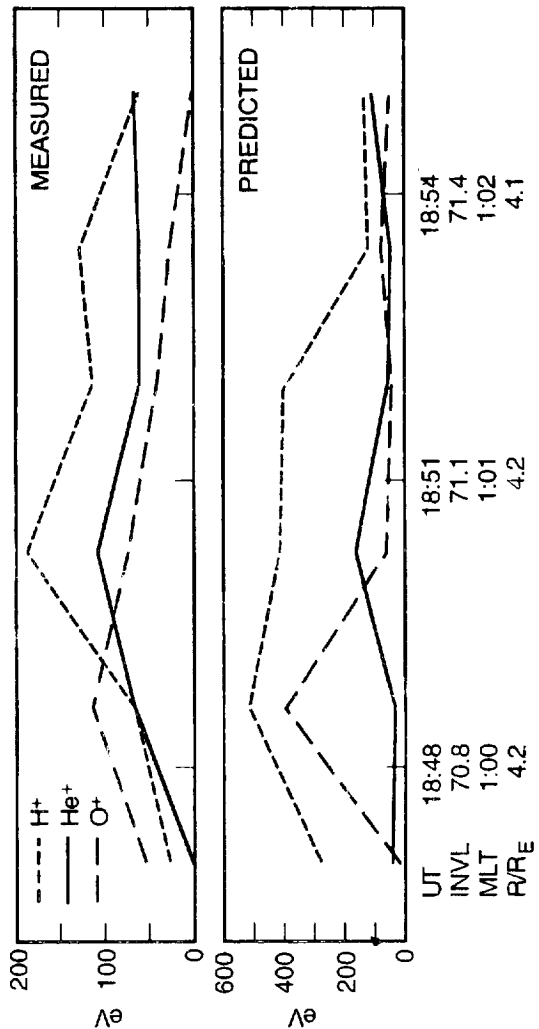
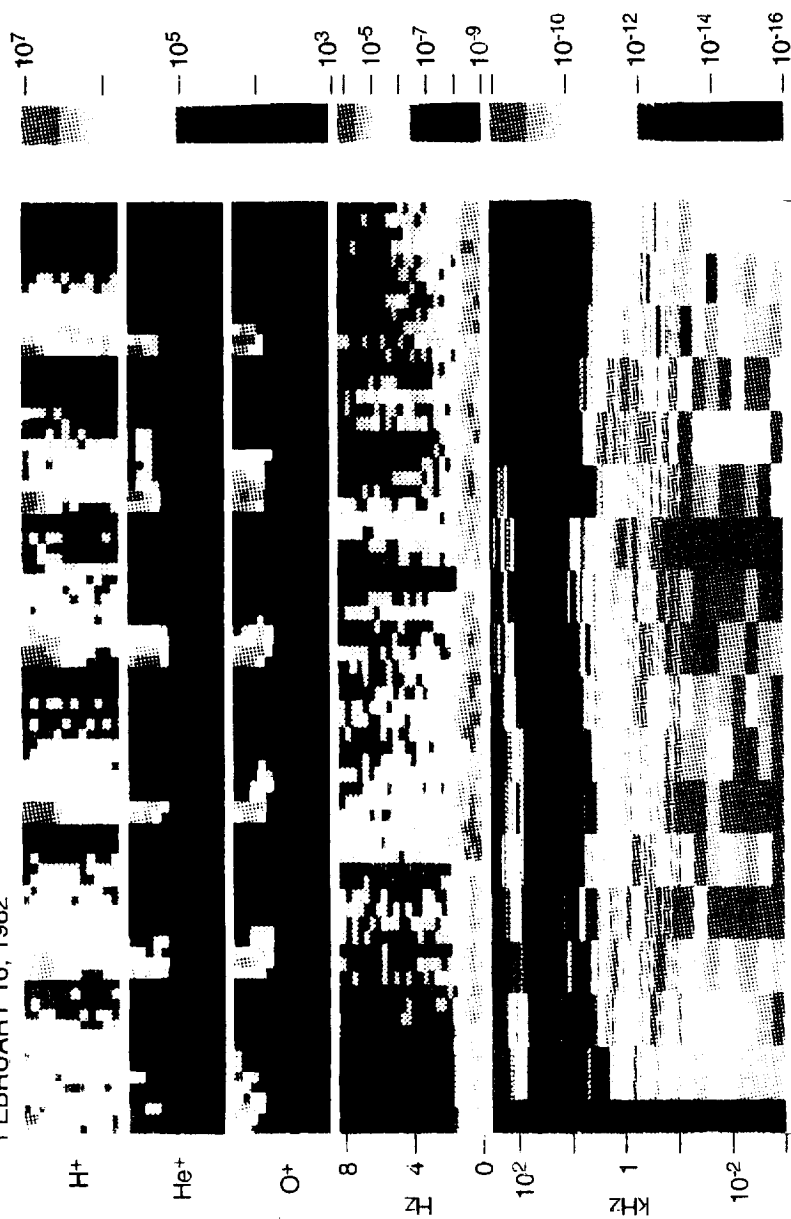


Plate 1

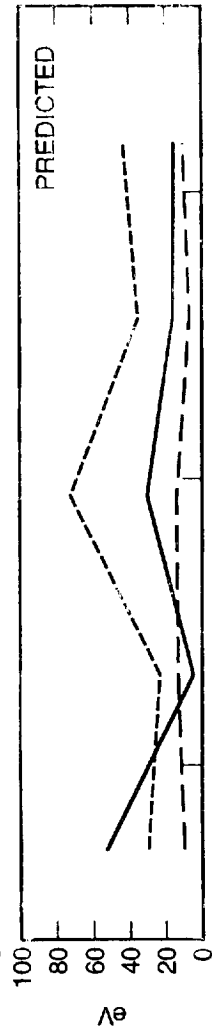
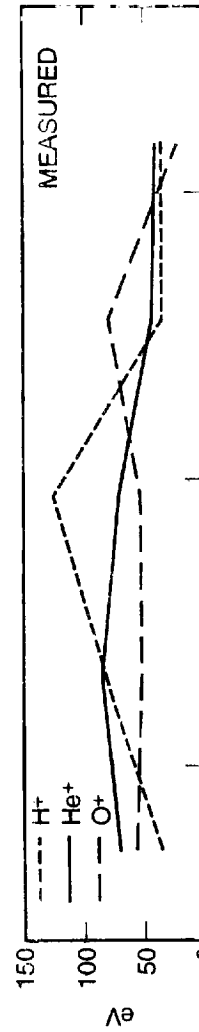


FEBRUARY 16, 1982





APRIL 21, 1982



UT	00:06	00:09	00:12
INVL	61.1	61.3	61.5
MLT	20:58	20:58	20:59
R/R <sub>E</sub>	4.3	4.3	4.3





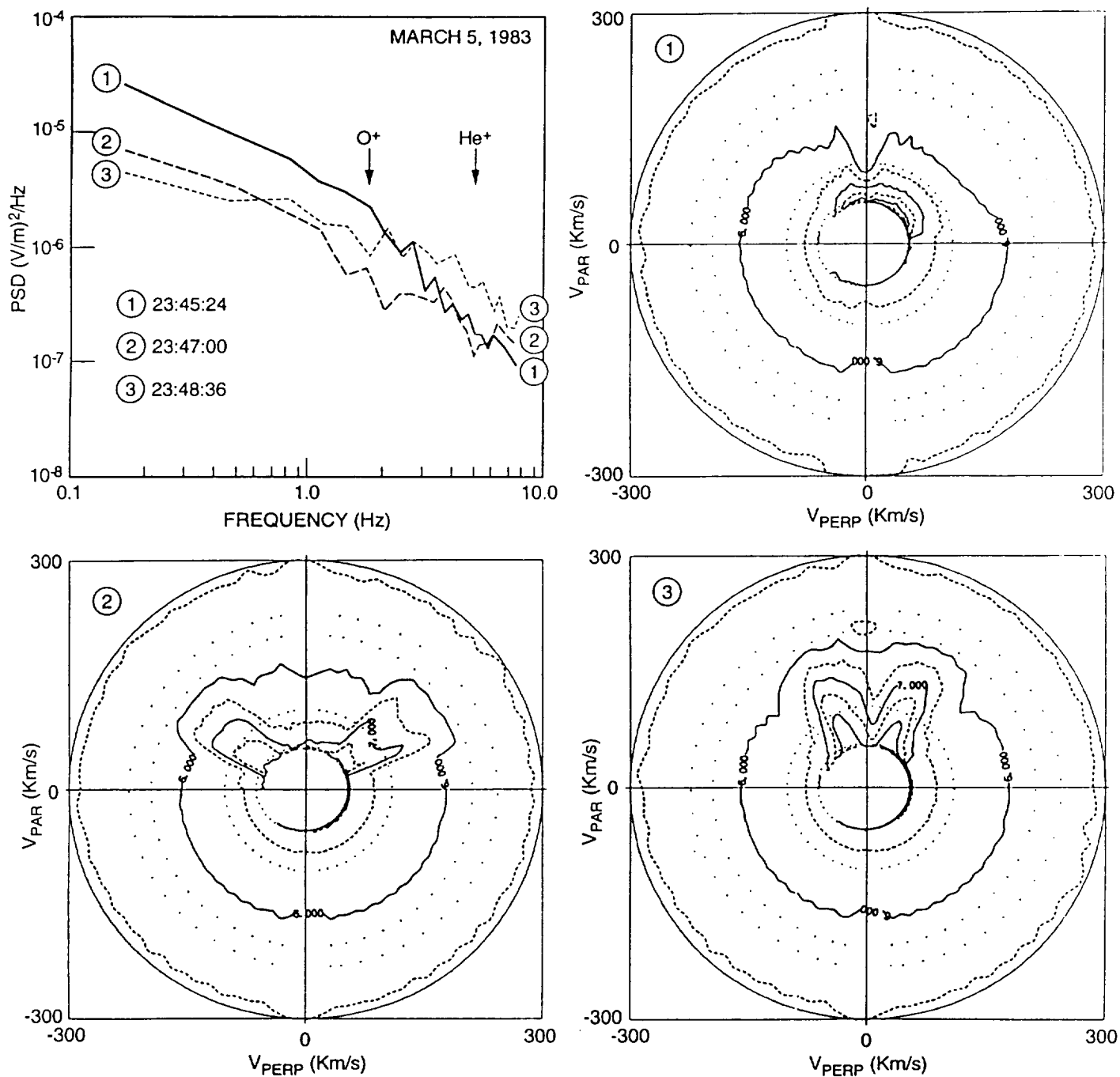


Figure 1

